Maximum Eigenvalue Matrix CFAR Detection Using Pre-Processing in Sea Clutter

WENJING ZHAO[ID], **(Student Member, IEEE), AND MINGLU JIN**[ID], **(Member, IEEE)**

School of Information and Communication Engineering, Dalian University of Technology, Dalian 116024, China

Corresponding author: Minglu Jin (mljin@dlut.edu.cn)

ABSTRACT For the pulse Doppler radar system with short pulse sequence, maximum eigenvalue-based matrix CFAR detector (MEMD) provides an effective solution to the problem of detecting moving targets in the background of K distribution sea clutter when the target Doppler frequency is within clutter spectrum. However, its performance is inferior to adaptive normalized matched filter method (ANMF) when the target Doppler frequency heavily deviates from the clutter spectrum. In essence, the reason for the better performance of ANMF method is the clutter is effectively suppressed by whitening and matched filter. Motivated by this, the fusion idea of eigenvalue detection and pre-processing via fast Fourier transform is considered taking advantage of the priori information of target steering vector. A pre-processing-based maximum eigenvalue matrix CFAR detection (P-MEMD) method is proposed to suppress the influence of clutter on detection performance. Finally, the numerical experimental results based on simulated data and real sea clutter data show that the proposed method achieves better detection performance and robustness than some conventional methods.

INDEX TERMS Moving target detection, pre-processing, sea clutter.

I. INTRODUCTION

The effective and robust detection for moving target in sea clutter is always an important and challenging task for maritime radar detection, which is meaningful for both military and civilian. In general, sea clutter presents non-Gaussian and non-linear characteristics, so that it has serious impact on moving target detection [1], [2]. To this end, much attention has been paid to how to suppress sea clutter so as to improve the detection performance [3].

The coherent detection methods using local power of echo and Doppler information are the commonly utilized to deal with the problem of moving target detection in sea clutter. For example, the cell averaging based on fast Fourier transform (FFT-CA) constant false alarm detection (CFAR) method is widely used employing the Doppler filter banks to improve clutter rejection. The FFT-CA method achieves good detection performance in the case of no energy leakage and high Doppler resolution. Take some practical scenarios into consideration, the clutter velocity dispersion caused by internal movement, radar platform movement, and wind speed, which results in Doppler frequency broadening of clutter spectrum [4]. In addition, to meet the new requirements

and challenges from system reaction time, utilizing short Doppler bursts with few of pulses is the antagonistic way to relax time budget [5]. However, for short pulse sequence, the Doppler resolution is poor and the signal component will exists in other filters when the target Doppler frequency cannot completely match the central frequency of the Doppler filter bank, which leads to energy leakage [6]. FFT-CA will suffer from the integration loss with respect to short pulse sequence and degraded detection performance for the case of clutter spectrum broadening, energy leakage of Doppler filter banks and low Doppler resolution [7]. Some other coherent detection methods were proposed to improve detection performance. More specifically, Kelly proposed the matched filter (MF) method that achieves satisfactory detection performance in the color Gaussian noise environment. Nevertheless, it requires the clutter covariance matrix to be known [8]. To deal with the case of unknown clutter covariance matrix, adaptive matched filter (AMF) method firstly uses clutter data of reference cells to estimate the clutter covariance matrix, and then carries out the coherent matched detection for the cell of under test (CUT) [9]. Subsequently, the normalized matched filter (NMF) and adaptive normalized matched filter (ANMF) methods came into being for the variation of clutter energy of reference cells in the background of compound Gaussian clutter [10], [11]. The ANMF method improves the

integration gain by accumulating multiple samples, so as to obtain better detection performance. However, the ANMF method relies on the clutter covariance matrix estimation, which promotes the research on clutter covariance matrix estimation under different conditions [12], [13]. For K distribution clutter environment, [14] proposed a suboptimal α-adaptive matched filter (α-AMF) algorithm to reduce the computational complexity of optimal coherent K-distributed detector (OKD). The detection performance of α-AMF is close to the OKD method when the ratio between the number of reference cells and the length of the coherent pulse train tends to infinity. While the detection performance of α-AMF is degraded when the ratio between the number of reference cells and the length of coherent pulse train is small.

All the above methods are based on the assumption that the target steering vector is known. If the steering vector is unknown or mismatched, then the detection performance of these methods will be degraded [15], [16]. For the case of unknown target steering vector, [17], [18] proposed the generalized likelihood ratio test (GLRT) detection method in Gaussian and compound Gaussian environment, as well as studied the influence of mismatched steering vector on detection performance. In addition, the totally blind matrix CFAR detector based on information geometry obtains good detection performance for the problem of detecting moving target in sea clutter [19]–[22]. It transforms the target detection problem into a geometric problem on matrix manifold, which overcomes the shortcomings of traditional FFT-CA method under the condition of short pulse sequence. While the kind of geometrical methods cost heavy computational complexity. The maximum eigenvalue based matrix CFAR detector (MEMD) is given to reduce computational complexity [23]. It achieves superior detection performance when the target Doppler spectrum overlaps with the clutter spectrum. However, its performance is inferior to ANMF when the target Doppler frequency removes from the clutter spectrum. The main reason is that ANMF method is a coherent method, which utilizes whitening and matched filter to suppress clutter. While MEMD method, as an incoherent method, cannot compensate the phase fluctuation resulting in low integration gain and degraded detection performance. Therefore, for the case of short pulses, it is very necessary to design a more robust CFAR detection algorithm with superior detection performance especially when the target spectrum is separated from the clutter spectrum. Motivated by this, we expect to enhance the detection performance of MEMD by using phase information or other ways to improve signal-to-clutter ratio (SCR) under the premise of ensuring CFAR property.

This paper considers the problem of moving target detection in the background where clutter and noise exist simultaneously. The combined idea of eigenvalue detection and pre-processing is adopted to weaken the influence of clutter on the detection performance as well as improve the detection performance of MEMD especially when target spectrum separates from the clutter spectrum. It is a technical difficulty to design an effective pre-processing mechanism.

The pre-processing via fast Fourier transform (FFT) based maximum eigenvalue matrix CFAR detector (P-MEMD) is proposed to improve integration gain using the prior information of target steering vector. The pre-processing process utilizing the phase information can suppress the clutter as well as this operation effectively cope with the performance degradation problem of the MEMD method when the target spectrum is separated from the clutter spectrum. In addition, the constant false alarm rate property of the proposed method with respect to clutter covariance matrix is analyzed. Compared with the conventional ANMF method and MEMD, the proposed method achieves better detection performance not only in the strong clutter environment, but also when the target Doppler frequency removes from the clutter spectrum. It indicates that the proposed method is more robust for the case of small bunch of pulses.

The structure of this paper is arranged as follows: the detection model of moving target is considered in Section II; Section III reviews two classical coherent methods, that is FFT-CA and ANMF. And then pre-processing based maximum eigenvalue detection method is proposed. In Section IV, the effectiveness of the proposed method is verified by simulation experiments on simulation data and real sea clutter data. Section V gives the conclusion.

A. ABBREVIATIONS AND ACRONYMS

A lot of notations adopted in this paper are listed as the following: scalars r, vectors $\mathbf{r}$ and matrices $\mathbf{R}$ are expressed by math italic, lowercase bold and uppercase bold, respectively. The complex conjugate and conjugate transpose operators are denoted as $(\cdot)^*$ and $(\cdot)^H$, respectively. $\lambda_{\max}(\cdot)$ means the maximum eigenvalue of a matrix. Curved inequality $\succ$ means that a matrix is positive definite. $U(M)$ stands for the set of all $M \times M$ unitary matrices. $\| \cdot \|_2$ means the spectral norm of a matrix. $tr(\cdot)$ denotes the trace of matrix, $diag(\cdot)$ represents taking the diagonal elements of a matrix and creating a new column vector.

II. PROBLEM FORMULATION

Formally, the problem of detecting radar moving target in the background of sea clutter plus noise can be represented by the following binary hypothesis model [23], [24]:

$$\begin{cases} H_0 : \mathbf{r} = \mathbf{c} + \mathbf{n} \\ H_1 : \mathbf{r} = a\mathbf{p} + \mathbf{c} + \mathbf{n} \end{cases} \quad (1)$$

where $\mathbf{r} \in \mathbb{C}^M$ is the M dimensional observation data vector of cell under test (CUT), referred to primary data. Under the null hypothesis, the CUT contains clutter $\mathbf{c}$ and Gaussian noise $\mathbf{n}$. The noise cannot be neglected in some practical scenarios especially in noise dominated Doppler regions at low grazing angle. Another hypothesis indicates that the CUT contains a target echo $a\mathbf{p}$ plus clutter $\mathbf{c}$ and noise $\mathbf{n}$, where a is the complex signal amplitude, $\mathbf{p}$ is the target steering vector with component of $\exp(j2\pi(m-1)f_d/f_r), m = 1, \ldots, M$. f_d stands for the target Doppler frequency, f_r represents pulse repetition frequency.
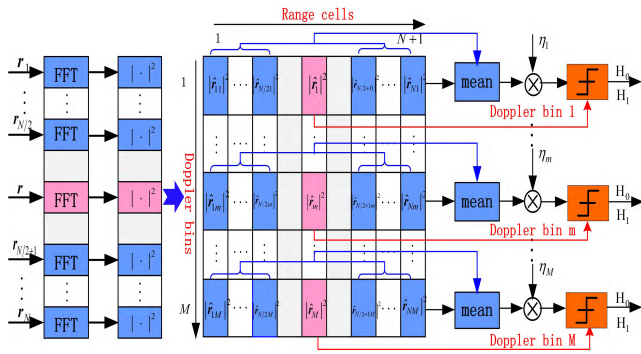
FIGURE 1. The block diagram of FFT-CA method.

In practice, the statistical characteristic of sea clutter gradually deviates from Gaussian distribution for high resolution radar system. Some literatures have shown that the compound Gaussian model can reflect the backscattering process of clutter and accurately model the statistical characteristics of sea clutter [25]. Clutter can be regarded as the product of the speckle component obeying the complex Gaussian distribution and the non-negative texture component. Formally, clutter is expressed as $\mathbf{c} = \sqrt{\tau}\mathbf{x}$. The speckle component $\mathbf{x}$ is zero-mean complex circular Gaussian vector with covariance matrix of $\mathbf{M} = E(\mathbf{x}\mathbf{x}^H)$. Additionally, covariance matrix is positive definite, i.e. $\mathbf{M} \succ \mathbf{0}$. Sea clutter follows K distribution, generalized Pareto distribution and inverse Gaussian Compound Gaussian distribution (IG-CG) when texture component τ follows Gamma distribution, inverse Gamma distribution and inverse Gaussian distribution, respectively. These three kinds of models accurately model the statistical characteristics of sea clutter under different conditions [26], [27]. In this paper, we assume that the clutter obeys the K distribution, whose amplitude statistical probability density function is expressed as follows:

$$f_K(c) = \frac{2\gamma}{\Gamma(\nu)} (\frac{\gamma c}{2})^\nu K_{\nu-1}(\gamma c) \qquad (2)$$

where γ and ν represent the scale parameter and shape parameter of K distribution, respectively. $\Gamma(\cdot)$ is Gamma function; $K_{\nu-1}(\cdot)$ is the second modified Bessel function of order $\nu - 1$.

III. PRE-PROCESSING BASED MAXIMUM EIGENVALUE MATRIX CFAR DETECTOR

This section firstly introduces two widely used solutions (i.e. FFT-CA and ANMF) to the detection problem (1), and then pre-processing based matrix CFAR detector is designed.

A. THE CLASSICAL CFAR DETECTORS

FFT-CA method is a classical detection method for the problem (1), whose block diagram is shown in Fig. 1. It is assumed that M pulses are transmitted in a coherent processing interval (CPI). As customary, we suppose that a set of N secondary data that is free of signal components in the cells adjacent to CUT is available. The in-phase and quadrature components of the echo signal are sampled, resulting in a complex matrix

of M rows (pulses) and $N + 1$ columns (range cells). The received data of CUT and the reference cells are denoted as $\mathbf{r}, \mathbf{r}_1, \ldots, \mathbf{r}_N$, respectively. It is assumed that $\mathbf{r}_1, \ldots, \mathbf{r}_N$ share the same covariance matrix with the clutter plus noise vector in the CUT. The detailed procedure of FFT-CA method is reviewed as follows [28], [29]:

- The fast Fourier transform (FFT), a computationally efficient way of implementing a bank of bandpass filters, is performed on received data in each range cell. Each DFT coefficient is viewed as the output from a Doppler filter. The outputs of FFT transform form a matrix of M rows (Doppler bins) and $N + 1$ columns (range cells).
- Calculate the squared magnitude of the FFT outputs in CUT and reference cells. The data of CUT and adjacent reference cells in the each Doppler bin are denoted as $|\widehat{r}_m|^2, |\widehat{r}_{1m}|^2, \ldots, |\widehat{r}_{Nm}|^2, m \in 1, \ldots, M$, respectively.
- Estimate the average power of clutter using the data of reference cells in each Doppler bin. The average power of clutter in each Doppler bin is given by $\frac{1}{N}\sum_{i=1}^{N}|\widehat{r}_{im}|^2, m \in 1, \ldots, M$.
- Compare the spectral power $|\widehat{r}_m|^2$ of CUT with the product of the power sum of the reference cells and threshold factor η_m selected to achieve the desired false alarm rate in each Doppler bin. And then a decision is made that a target is present in the CUT. It is noted that if the target Doppler frequency is known, then we can perform the processing with one Doppler bin alone.

Another conventional coherent method for the detection problem (1) is adaptive normalized matched filter (ANMF), whose detection statistics is expressed as follows:

$$\frac{\left|\mathbf{p}^H \hat{\mathbf{R}}_\mathbf{r}^{-1} \mathbf{r}\right|^2}{\left(\mathbf{p}^H \hat{\mathbf{R}}_\mathbf{r}^{-1} \mathbf{p}\right)\left(\mathbf{r}^H \hat{\mathbf{R}}_\mathbf{r}^{-1} \mathbf{r}\right)} \underset{H_0}{\overset{H_1}{\gtrless}} \eta, \qquad (3)$$

where the covariance matrix $\hat{\mathbf{R}}_\mathbf{r}$ is estimated using the data of reference cells. $\mathbf{r}$ denotes the received data of CUT, $\mathbf{p}$ is the target steering vector.

A long-time coherent integration technique is one of the most useful methods for improving radar detection ability. FFT-CA method obtains good detection performance under the condition of long pulse train. However, the amplitude modulation and Doppler frequency spread of the target signal over a long integration time are unavoidable. The antagonistic way is to utilize short Doppler bursts with few of pulses to avoid amplitude modulation and Doppler frequency spread. While energy leakage of Doppler filter banks and low Doppler resolution emerge in the case of short pulse sequences. The performance of FFT-CA is seriously degraded due to small bunch of accumulated pulses. The matrix CFAR detection method based on information geometry was proposed to overcome these shortcomings [19]. Nevertheless, its heavy computational complexity limits its application in practical scenarios. The maximum eigenvalue
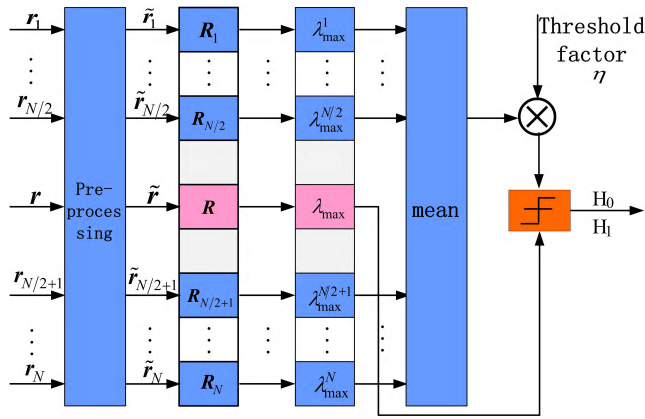
FIGURE 2. The block diagram of P-MEMD method.

FIGURE 3. The flowchart of pre-processing process.

based detection method (MEMD) is designed to achieve better performance with lower computational complexity in the strong clutter region [23]. While the detection performance of MEMD is inferior to the classical ANMF method when the target Doppler frequency heavily deviates from the clutter spectrum. As an incoherent detector, MEMD does not take full advantage of the target Doppler information resulting in low integration gain. This paper considers adding pre-processing process to weaken the influence of clutter on detection performance. An enhanced maximum eigenvalue based matrix CFAR detection method is proposed to improve detection performance especially when target Doppler frequency removes from the clutter spectrum.

B. PRE-PROCESSING BASED MAXIMUM EIGENVALUE MATRIX CFAR DETECTOR

The complex sea clutter environment has great influence on radar moving target detection. The pre-processing based maximum eigenvalue matrix detector (P-MEMD) method combines the frequency domain coherent integration with the maximum eigenvalue method. P-MEMD weakens the influence of clutter using the prior information of target steering vector and further improves the detection performance. Fig. 2 shows the block diagram of the proposed P-MEMD method, which involves five steps: Preprocess the received data of CUT and reference cells; Calculate the covariance matrix of each range cell; Solve the maximum eigenvalue of covariance matrix in each range cell; Calculate the arithmetic mean of maximum eigenvalues in reference cells; Make a decision. In what follows, the detailed procedure of P-MEMD method will be explained.

Let $\{\mathbf{r}, \mathbf{r}_1, \dots, \mathbf{r}_N\}$ is the received data matrix, which is partitioned into the primary and secondary data arrays. Here, $\mathbf{r}$ denotes the M dimensional received data of CUT (primary data), $\mathbf{r}_1, \dots, \mathbf{r}_N$ represent the received data consisting of clutter and noise in reference cells (secondary data).

● **Pre-processing:**

Pre-processing is implemented on the received data in the frequency domain as FFT-CA. Fig. 3 depicts the flowchart
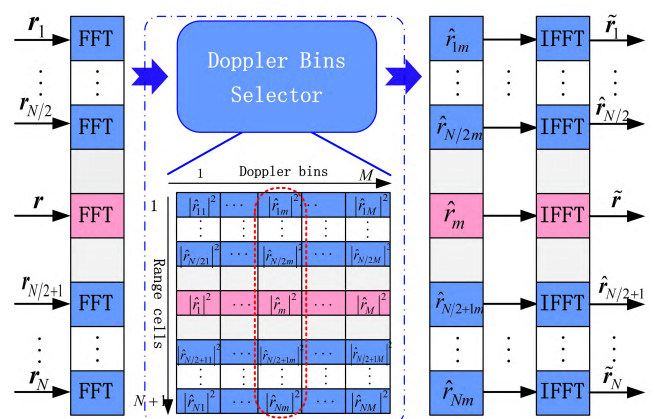
of the pre-processing process. The detailed steps of pre-processing process are explained as follows:

(i) As a common tool for signal processing, fast Fourier transform (FFT) is simple and can reduce computation and hardware consumption. The FFT is performed on the received data $\{\mathbf{r}, \mathbf{r}_1, \dots, \mathbf{r}_N\}$ of CUT and reference cells, which decomposes the received vector into multiple Doppler bins. FFT transform corresponds to multiple coherent integrators, which improves the integration gain. The outputs of FFT transform in the CUT and the reference cells constitute a matrix of $N + 1$ columns (range cells) and M rows (Doppler bins).

(ii) As shown in the blue dotted box in Fig. 3, the data of a single Doppler bin is selected using the Doppler bins selector from the data matrix obtained in step (i). The Doppler bins selector is designed under the assumption that the target Doppler steering vector is perfectly known. Therefore, at the design stage, the Doppler bin selected is easy to determined according to the target Doppler frequency. The data of the same Doppler bin for the reference cells are selected when the Doppler bin of the CUT is determined. This operation effectively suppress the clutter.

The Doppler frequency of moving target should be known to perform the accurate pre-processing. However, the actual speed of the moving target cannot be known in advance, that is, the target Doppler frequency is unknown. Therefore, it is necessary to design a different Doppler bins selector covering the whole Doppler range and perform pre-processing. The signal energy after FFT transformation should concentrate in a certain Doppler bin. Motivated by this, the Doppler bins selector is implemented employing the peak search process within a certain Doppler frequency range to find the Doppler bin with the maximum energy, that is, the Doppler bin where the target may locates in. The detailed search process is described as follows:

The squared magnitudes of the FFT outputs in step (i) are calculated to form a new data matrix of $N + 1$ rows and M columns. The data of CUT and adjacent reference cells in the each Doppler bin are denoted as $|\hat{r}_m|^2, |\hat{r}_{1m}|^2, \dots, |\hat{r}_{Nm}|^2, m \in 1, \dots, M$, respectively.

And then the peak value of squared magnitudes of FFT outputs in CUT is searched to determine the Doppler bin where the peak value is located. The data in the selected Doppler bin (as shown in the red oval dotted box in Fig. 3) of CUT and adjacent reference cells are denoted as $|\hat{r}_m|^2, |\hat{r}_{nm}|^2, m \in 1, \ldots, M, n \in 1, \ldots, N$, respectively. The data in the selected Doppler bin forms an $N + 1$ dimensional vector.

(iii) The inverse FFT (IFFT) transform is respectively carried out on the each component representing the outputs of step (ii) in CUT and reference cells. Taking the data in CUT as an example, the outputs of step (ii) in CUT is converted into an M dimensional vector by setting other Doppler bins than the selected bin to 0, which is expressed as $[0, \cdots, \hat{r}_m, \cdots 0], m \in 1, \ldots, M$. The data of the reference cells are processed in the same way, and then the IFFT transform is implemented to obtain $N + 1$ vectors with dimension of M. The outputs of IFFT transform form a new data matrix $\{\tilde{\mathbf{r}}, \tilde{\mathbf{r}}_1, \ldots, \tilde{\mathbf{r}}_N\}$, where $\tilde{\mathbf{r}}$ denotes the transformed data of CUT, $\{\tilde{\mathbf{r}}_1, \ldots, \tilde{\mathbf{r}}_N\}$ represent the transformed data of reference cells, each complex value of this matrix stands for a time sample of the filtered data.

● **Calculate the covariance matrix:**

Calculate the covariance matrices of the filtered data in CUT and reference cells, and denote them as $\mathbf{R}, \mathbf{R}_1, \ldots, \mathbf{R}_N$, respectively. Experimental data indicate that the clutter amplitude probability density function (apdf) can be generally modeled as a compound-Gaussian process at low grazing angles. The model degenerates into a spherically invariant random process especially for time series observed on sufficiently short time intervals [30]. This paper considers the case of short pulses, which means the clutter satisfies wide-sense stationary property. References [4], [11], and [30]–[32] showed that the covariance matrix possesses Toeplitz structure under the assumption of wide-sense stationary clutter. The Toeplitz matrix can be used to model the correlation of periodic stationary processes in periodic time series. With limited sample support, the structural covariance matrix can reduce the estimation complexity, which is widely used in radar imaging, target detection, and communication system. Hence, it is a reasonable and advantageous assumption that clutter covariance matrix possesses the Toeplitz structure. The Toeplitz matrix can be estimated using empirical maximum likelihood and eigenvalue decomposition based method [31]–[33]. The covariance matrices with Hermitian Toeplitz structure are calculated according to correlation coefficients and given by the following form [26]:

$$\mathbf{R_r} = \mathbb{E}[\tilde{\mathbf{r}}\tilde{\mathbf{r}}^H] = \begin{bmatrix} a_0 & a_1 & \cdots & a_{M-1} \\ a_1^* & a_0 & \cdots & a_{M-2} \\ \vdots & \vdots & \ddots & \vdots \\ a_{M-1}^* & a_{M-2}^* & \cdots & a_0 \end{bmatrix} \quad (4)$$

where a_k is referred to the correlation coefficient and is expressed as follows:

$$a_k = \mathbb{E}[\tilde{r}_i \tilde{r}_{i+k}^*], 0 \leq k \leq M - 1, 1 \leq i \leq M.$$

However, the statistical covariance matrix (4) is difficult to acquire due to a limited number of samples. In general, the correlation coefficient of the received data is calculated utilizing the averaging over time instead of statistical expectation. The correlation coefficient is given by

$$\hat{a}_k = \frac{1}{M} \sum_{m=0}^{M-1-|k|} \tilde{r}(m)\tilde{r}^*(m+k), |k| \leq M - 1. \quad (5)$$

● **Solve the maximum eigenvalue:**

Solve the maximum eigenvalues of covariance matrices in CUT and reference cells by eigenvalue decomposition. The maximum eigenvalues in the potential target cell and reference cells are denoted as $\lambda_{\max}, \lambda_{\max}^1, \ldots, \lambda_{\max}^N$, respectively.

● **Calculate the arithmetic mean:**

The arithmetic mean of the maximum eigenvalues in the reference cells is calculated, which is expressed as

$$\frac{1}{N} \sum_{i=1}^{N} \lambda_{\max}^i.$$

● **Make a decision:**

The test statistic of P-MEMD method is expressed in the form:

$$\frac{\lambda_{\max}}{\frac{1}{N} \sum_{i=1}^{N} \lambda_{\max}^i} \underset{H_0}{\overset{H_1}{\gtrless}} \eta. \quad (6)$$

It is judged as the target presents in the CUT when the test statistic is greater than the threshold η; otherwise, it indicates the target absents in CUT.

P-MEMD method implements pre-processing by performing FFT transform on the received echo data in CUT and reference cells. Pre-processing is performed in the frequency domain under the assumption that the target steering vector is perfectly known. The peak search process is performed for the scenario with unknown target Doppler frequency. The clutter can be effectively suppressed if the center frequency of clutter deviates from the target Doppler frequency. And then it utilizes the maximum eigenvalue as test statistic, which can achieve better detection performance in the case of short pulse sequences. Subsequent simulation results show that P-MEMD achieves better detection performance not only in the strong clutter environment, but also in the scenario where target Doppler frequency removes from the clutter spectrum.

C. CFAR PROPERTY OF P-MEMD DETECTOR

Constant false alarm rate property is an desired property pursued by adaptive detectors. In essence, CFAR detection refers to the fact that false alarm probability is independent of some nuisance parameters related to the clutter such as clutter covariance matrix. However, the analytical expression of false alarm probability is difficult to obtain due to the intricate mathematical description of clutter statistical characteristics. The principle of invariance provides a new means for the proof of CFAR property. Some literatures resorted

to principle of invariance to study the CFAR property of some detectors [34]–[38]. In this paper, the CFAR property of the proposed method with respect to nuisance parameter (clutter covariance matrix in our paper) is analyzed using the framework of invariance principle. This subsection firstly reviews some definitions and property used in this paper and then considers the CFAR property of the proposed method with respect to clutter covariance matrix.

Let $\mathcal{G} \in U(M)$ be a finite unitary group, $\mathbf{X}$ is data with PDF $f(\mathbf{X}; \theta)$, where θ is the unknown parameter. If the PDF of $\mathbf{Y} = g(\mathbf{X})$ under group transformation $g \in \mathcal{G}$ does not depend on unknown parameter θ, then the PDF distribution of $\mathbf{Y}$ is called the standard type distribution, and g is the standard type transformation. An important property of the invariant principle is described as follows:

Property 1: Let θ is an unknown parameter, if $T(\mathbf{X})$ is the invariant statistic about $\mathcal{G}$, and there is a standard transformation $g \in \mathcal{G}$, then the false alarm probability of the binary hypothesis with test statistic $T(\mathbf{X})$ is independent on unknown parameter θ [35].

The Property 1 indicates that the proof idea of CFAR property is to ensure the distribution of test statistics is independent of some nuisance parameters under the appropriate group transformation $g \in \mathcal{G}$. Employing this proof framework, we will demonstrates that P-MEMD detector possesses the CFAR property with respect to clutter covariance matrix.

The test statistics of P-MEMD is expressed in the form:

$$\frac{\lambda_{\max}(\mathbf{R})}{\frac{1}{N} \sum_{i=1}^{N} \lambda_{\max}^{i}(\mathbf{R}_i)} \quad (7)$$

where the covariance matrices $\mathbf{R}$ and $\mathbf{R}_i$ of CUT and reference cells are calculated using equation (4) and equation (5).

The correlation coefficient (5) can be expressed as follows:

$$\hat{a}_k = \frac{1}{M} \sum_{m=1}^{M-k} \widetilde{\mathbf{r}}(m) \widetilde{\mathbf{r}}^*(m+k)$$

$$= \frac{1}{M}[\widetilde{\mathbf{r}}(1), \widetilde{\mathbf{r}}(2), \cdots, \widetilde{\mathbf{r}}(M-k)] \begin{bmatrix} \widetilde{\mathbf{r}}^*(1+k) \\ \widetilde{\mathbf{r}}^*(2+k) \\ \vdots \\ \widetilde{\mathbf{r}}^*(M) \end{bmatrix} \quad (8)$$

Furthermore, equation (8) is equivalent to

$$\hat{a}_k = \frac{1}{M}[\widetilde{\mathbf{r}}(1), \widetilde{\mathbf{r}}(2), \cdots, \widetilde{\mathbf{r}}(M)] \cdot \mathbf{F}_k \cdot \begin{bmatrix} \widetilde{\mathbf{r}}^*(1) \\ \widetilde{\mathbf{r}}^*(2) \\ \vdots \\ \widetilde{\mathbf{r}}^*(M) \end{bmatrix}, \quad (9)$$

where

$$\mathbf{F}_1 = \begin{bmatrix} 0 & 1 & 0 & \cdots & 0 \\ 0 & 0 & 1 & \cdots & 0 \\ \vdots & \vdots & \vdots & \ddots & 0 \\ 0 & 0 & 0 & \cdots & 1 \\ 0 & 0 & 0 & \cdots & 0 \end{bmatrix}, \quad \mathbf{F}_k = \mathbf{F}_1^k.$$

The corresponding covariance matrix calculated by correlation coefficient is expressed in the form

$$\hat{\mathbf{R}} = \frac{1}{M} \begin{bmatrix} \widetilde{\mathbf{r}}^H \widetilde{\mathbf{r}} & \widetilde{\mathbf{r}}^H \mathbf{F}_1 \widetilde{\mathbf{r}} & \cdots & \widetilde{\mathbf{r}}^H \mathbf{F}_{M-1} \widetilde{\mathbf{r}} \\ \widetilde{\mathbf{r}}^H \mathbf{F}_1^H \widetilde{\mathbf{r}} & \widetilde{\mathbf{r}}^H \widetilde{\mathbf{r}} & \cdots & \widetilde{\mathbf{r}}^H \mathbf{F}_{M-2} \widetilde{\mathbf{r}} \\ \vdots & \vdots & \ddots & \vdots \\ \widetilde{\mathbf{r}}^H \mathbf{F}_{M-1}^H \widetilde{\mathbf{r}} & \widetilde{\mathbf{r}}^H \mathbf{F}_{M-2}^H \widetilde{\mathbf{r}} & \cdots & \widetilde{\mathbf{r}}^H \widetilde{\mathbf{r}}. \end{bmatrix} \quad (10)$$

where $\widetilde{\mathbf{r}} = [\widetilde{\mathbf{r}}(1), \widetilde{\mathbf{r}}(2), \cdots, \widetilde{\mathbf{r}}(M)]$. The maximum eigenvalue of covariance matrix $\hat{\mathbf{R}}$ for $M = 2$ is given by

$$\widetilde{\mathbf{r}}^H \widetilde{\mathbf{r}} + \left| \widetilde{\mathbf{r}}^H \mathbf{F}_1 \widetilde{\mathbf{r}} \right|. \quad (11)$$

The maximum eigenvalue of covariance matrix $\hat{\mathbf{R}}$ for $M = 3$ is expressed as follows:

$$\left| \widetilde{\mathbf{r}}^H \left(\mathbf{I} + \frac{1}{2} \mathbf{F}_1 \mathbf{F}_1^H + \frac{1}{2} \left(\left(\mathbf{F}_1^2 \left(\mathbf{F}_1^H \right)^2 + 8 \mathbf{F}_1 \mathbf{F}_1^H \right)^{1/2} \right) \right) \widetilde{\mathbf{r}} \right|. \quad (12)$$

The analytic expression of the maximum eigenvalue of the covariance matrix $\hat{\mathbf{R}}$ is complicated when $M > 3$. The derivation and analysis show that the maximum eigenvalue of the covariance matrix $\hat{\mathbf{R}}$ can be expressed in this form $| \widetilde{\mathbf{r}} f(\mathbf{F}_1) \widetilde{\mathbf{r}}^H |$, where $f(\mathbf{F}_1)$ is a matrix function of $\mathbf{F}_1$ and is a positive definite matrix.

Furthermore, the test statistics is given by:

$$\frac{\left| \widetilde{\mathbf{r}}^H f(\mathbf{F}_1) \widetilde{\mathbf{r}} \right|}{\frac{1}{N} \sum_{i=1}^{N} \left| \widetilde{\mathbf{r}}_i^H f(\mathbf{F}_1) \widetilde{\mathbf{r}}_i \right|}. \quad (13)$$

Consider the following inner product in the form of a matrix trace [39]–[42], then formula (13) is converted to

$$\frac{\left| tr(\widetilde{\mathbf{r}} \widetilde{\mathbf{r}}^H f(\mathbf{F}_1)) \right|}{\frac{1}{N} \sum_{i=1}^{N} \left| tr(\widetilde{\mathbf{r}}_i^H \widetilde{\mathbf{r}}_i f(\mathbf{F}_1)) \right|}. \quad (14)$$

Under the null hypothesis, assume that the statistical covariance matrix of $\widetilde{\mathbf{r}}$ and $\widetilde{\mathbf{r}}_i$ is Σ, which is a positive definite Hermitian matrix. Thereby, the received data of CUT and reference cells can be whitened with $\Sigma^{-1/2}$ and expressed as the following [35]

$$\bar{\mathbf{r}} = \Sigma^{-1/2} \widetilde{\mathbf{r}},$$
$$\bar{\mathbf{r}}_i = \Sigma^{-1/2} \widetilde{\mathbf{r}}_i. \quad (15)$$

The vector $\bar{\mathbf{r}}$ and $\bar{\mathbf{r}}_i$ are zero-mean complex Gaussian vectors with covariance matrix $\mathbf{I}_M$, where $\mathbf{I}_M$ is identity matrix of order M. Using the formula (15), the formula (14) can be converted to

$$\frac{\left| tr(\Sigma^{1/2} \bar{\mathbf{r}} \bar{\mathbf{r}}^H \Sigma^{1/2} f(\mathbf{F}_1)) \right|}{\frac{1}{N} \sum_{i=1}^{N} \left| tr(\Sigma^{1/2} \bar{\mathbf{r}}_i \bar{\mathbf{r}}_i^H \Sigma^{1/2} f(\mathbf{F}_1)) \right|}. \quad (16)$$

Since $tr(\mathbf{AB}) = tr(\mathbf{BA})$, then formula (16) is expressed as follows:

$$\frac{\left|tr(\bar{\mathbf{r}}\bar{\mathbf{r}}^H \Sigma^{1/2} f(\mathbf{F}_1) \Sigma^{1/2})\right|}{\frac{1}{N}\sum_{i=1}^{N}\left|tr(\bar{\mathbf{r}}_i\bar{\mathbf{r}}_i^H \Sigma^{1/2} f(\mathbf{F}_1) \Sigma^{1/2})\right|}. \qquad (17)$$

In addition, $\Sigma^{1/2} f(\mathbf{F}_1) \Sigma^{1/2}$ is positive definite matrix, hence it can be diagonalized by a unitary transformation and is given by

$$\Sigma^{1/2} f(\mathbf{F}_1) \Sigma^{1/2} = \mathbf{V}\Lambda\mathbf{V}^H. \qquad (18)$$

For the sake of simplicity, let $\mathbf{A} = \bar{\mathbf{r}}\bar{\mathbf{r}}^H$, $\mathbf{A}_i = \bar{\mathbf{r}}_i\bar{\mathbf{r}}_i^H$. Put (18) into the formula (17), then formula (17) is converted to

$$\frac{tr(\mathbf{A}\mathbf{V}\Lambda\mathbf{V}^H)}{\frac{1}{N}\sum_{i=1}^{N} tr(\mathbf{A}_i\mathbf{V}\Lambda\mathbf{V}^H)}. \qquad (19)$$

Furthermore, the formula (19) is recast into

$$\frac{tr(\mathbf{V}^H\mathbf{A}\mathbf{V}\Lambda)}{\frac{1}{N}tr(\mathbf{V}^H\sum_{i=1}^{N}\mathbf{A}_i\mathbf{V}\Lambda)}. \qquad (20)$$

According to the definition of trace of matrix, the formula (20) is equivalent to

$$\frac{diag(\mathbf{V}^H\mathbf{A}\mathbf{V})^T diag(\Lambda)}{\frac{1}{N}\sum_{i=1}^{N} diag(\mathbf{V}^H\mathbf{A}_i\mathbf{V})^T diag(\Lambda)} = \frac{N \cdot diag(\mathbf{V}^H\mathbf{A}\mathbf{V})^T}{\sum_{i=1}^{N} diag(\mathbf{V}^H\mathbf{A}_i\mathbf{V})^T}. \qquad (21)$$

As shown in formula (21), $\mathbf{V}^H\mathbf{A}\mathbf{V}$ is a matrix whose columns are independent and identically distributed complex normal vectors with zero mean and covariance matrix $\mathbf{I}_M$. Under H_0, formula (21) indicates that the PDF of the test statistics is independent of clutter covariance matrix under the group transformation $\Sigma^{-1/2}\mathbf{V}$. In conclusion, the proposed P-MEMD method ensures the desirable CFAR property with respect to clutter covariance matrix.

In the following, some Monte Carlo simulation experiments are performed to validate the CFAR property of P-MEMD method in regard to clutter covariance matrix. Some simulation parameters are set as follows: the number of reference cells is 16, the size of pulse train is 8. The clutter covariance matrix can be modeled as following exponentially shaped form [12], [18], and [43]:

$$\Sigma = \sigma_c^2 \rho^{|i-k|} e^{j2\pi f_{dc}(i-k)} + \mathbf{I}, i, k = 1, \ldots, M \qquad (22)$$

where ρ is the one-lag correlation coefficient. ρ reflects the variation of the covariance matrix under the given σ_c^2 and f_{dc}, which can be utilized to show the change of false alarm probability with respect to different covariance matrix. Therefore, different correlation coefficient of covariance matrix is employed to assess the CFAR property of P-MEMD. Correlation coefficient is set to 0.1, 0.3, 0.5, 0.7 and 0.9. Fig. 4 shows the probability of false alarm versus threshold plots with respect to different correlation coefficient of
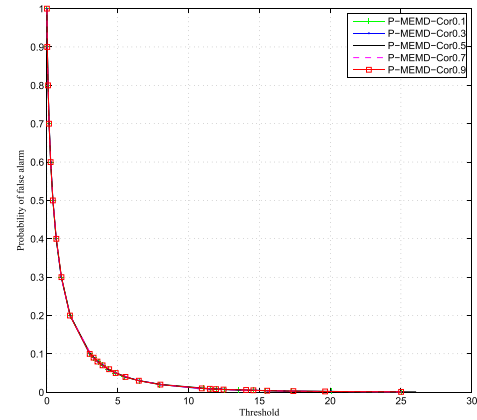

FIGURE 4. Probability of false alarm versus the detection threshold of P-MEMD method for different correlation coefficient of covariance matrix.

TABLE 1. Computational complexity of detection methods.

Algorithm	Covariance matrix	Basic operations: multiplication / addition
P-MEMD	YES	$(N+1)Mlog(M) + (N+1)M^3 + N$
MEMD	YES	$(N+1)M^3 + N$
KLD	YES	$M! + (N+3)M^3 + (N+1)M^2 + M$
ANMF	YES	$M^3 + 3M^2 + 3M + 2$
α-ANMF	YES	$M^3 + 3M^2 + 3M + 3$
FFT-CA	NO	$(N+1)Mlog(M) + 2N$

covariance matrix. As seen from Fig. 4, the curves completely coincide corresponding to different one-lag correlation coefficients. In other words, the false alarm rate is independent on the correlation coefficients. It further indicates that P-MEMD method possesses CFAR property with respect to clutter covariance matrix.

D. COMPUTATIONAL COMPLEXITY ANALYSIS

The computational complexity of an algorithm is generally related to its implementation, so the computation complexity of some special functions is not be considered in the complexity analysis. In what follows, we analyze the computational complexity of the proposed method using the total number of the multiplications and additions involved in an algorithm. This paper considers the computational complexity of the P-MEMD with other five kinds of methods: the adaptive normalized matched filtering method (ANMF), shape parameter dependent adaptive matched filtering method (α-ANMF), Kullback-Leibler divergence based matrix CFAR detector (KLD), maximum eigenvalue based matrix CFAR detector (MEMD) and FFT-CA method. Taking the MEMD method as an example, the MEMD only needs N addition operations, $N+1$ eigenvalue decomposition operations with complexity of M^3, therefore, the complexity of MEMD is $(N+1)M^3+N$. Table 1 summarizes the computational complexity of the proposed method and other algorithms, where M is the length of transmitted pulse train, N is the number of reference cells. As observed from Table 1, the computational complexity of the proposed method is lower than KLD algorithm. That is because it does not require matrix inverse operation. While the P-MEMD method costs slightly high computational complexity than ANMF, α-ANMF, FFT-CA,

and MEMD methods. Nevertheless, subsequent simulation experiments will show that P-MEMD method achieves superior detection performance than other aforementioned methods.

IV. SIMULATIONS AND DISCUSSIONS

In this section, the performance of P-MEMD method and some existing conventional detection methods are compared to verify the effectiveness of P-MEMD method through the simulation experiment based on simulation data and real clutter data. For comparison, the ANMF, α-ANMF, KLD, MEMD and FFT-CA methods are considered.

A. SIMULATION EXPERIMENTS ON SIMULATED DATA

In this paper, we assume that sea clutter follows K distribution, the shape parameter and scale parameter of K distribution are set as $\nu = 1, \gamma = 1$, respectively. The mean Doppler frequency of sea clutter is set to be 65Hz and the clutter spectrum broadening is adjusted by 3dB bandwidth. In some practical scenarios, the receiver noise is a factor that can not be neglected. Therefore, the effect of Gaussian white noise is also considered in this paper, and the clutter-to-noise ratio (CNR) is set to be 10dB. For the radar system with short pulse sequences, the detection of moving targets against sea clutter environment is intricate due to limited pulses to be accumulated. In this paper, it is assumed that the radar transmits 8 pulses in a CPI. The other parameters are set as follows: signal-to-clutter ratio (SCR) is set to be 0 dB to 20 dB. The pulse repetition frequency is 1000 Hz, the number of reference cells is 16. The false alarm probability is set to be 10^{-4}. In addition, the threshold is determined by Monte Carlo simulation as the theoretical representation of threshold is difficult to obtain. The samples of the test statistic under the null hypothesis H_0 are used to determine the decision threshold. According to the preset false alarm probability P_{fa}, $100/P_{fa}$ Monte Carlo simulation experiments are carried out to determine the threshold with sufficient precision at the false alarm.

The terrible cases of energy leakage under the condition of short pulse train and clutter spectrum broadening are discussed in this paper. Energy leakage is caused when the target Doppler frequency cannot completely match the central frequency of the Doppler filters bank. Energy leakage is serious especially when the target Doppler frequency is between two filters [6]. Several scenarios are considered by adjusting the 3dB bandwidth of sea clutter spectrum and target Doppler frequency. The following five simulation scenarios are summarized in Table 2, where "YES" and "NO" represent the presence and absence of clutter spectrum broadening and energy leakage, respectively. The fifth scenario in which the target spectrum is within the clutter spectrum is different from the first four scenarios.

The schematic diagram for the first 4 detection scenarios are depicted in Fig. 5. The yellow lines represent the clutter spectrum, the pink lines represent the target spectrum and blue shaded rectangles spaced apart in Doppler represents the

TABLE 2. Parameter setting for different detection scenarios.

Scenarios	clutter spectrum broadening	energy leakage	f_d	f_{dc}	W_{3dB}
1	NO	NO	142Hz	65Hz	40Hz
2	YES	NO	142Hz	65Hz	80Hz
3	NO	YES	215Hz	65Hz	40Hz
4	YES	YES	215Hz	65Hz	80Hz
5	YES	NO	65Hz	65Hz	80Hz

* f_d: target Doppler frequency;
  f_{dc}: mean Doppler frequency of sea clutter;
  W_{3dB}: 3dB bandwidth of clutter spectrum.

(a) scenario 1
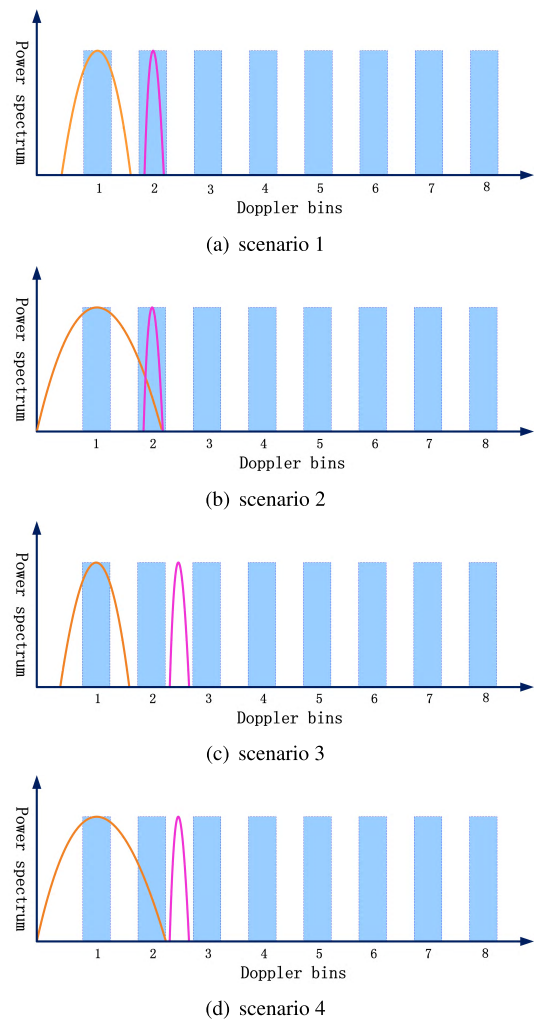
(b) scenario 2

(c) scenario 3

(d) scenario 4

FIGURE 5. A pictorial representation for the detection scenarios.

Doppler bin. The schematic diagram depicted in Fig. 5 just to make it clear to show the difference between the presence and absence of the clutter spectrum broadening and energy leakage. The simulation comparisons for the five cases are made, which are shown in Fig. 6 to Fig. 10, respectively.

As described in Fig. 6, the detection probability of P-MEMD method versus different SCRs is compared with that of ANMF, α-ANMF, KLD, MEMD and FFT-CA methods for the case (1). It can be seen from Fig. 6 that the proposed method is superior to the KLD, MEMD and FFT-CA methods in the scenario without clutter spectrum broadening
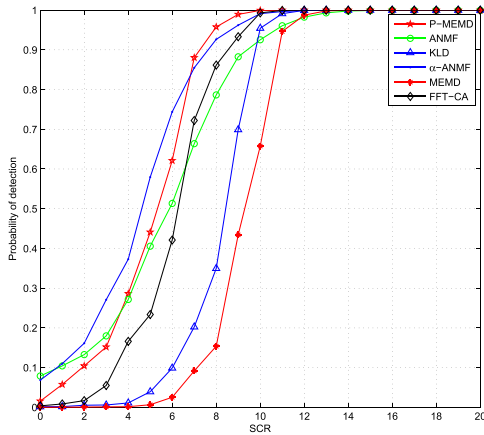
FIGURE 6. The detection performance comparison of P-MEMD, ANMF, α-ANMF, KLD, MEMD and FFT-CA methods in the scenario without clutter spectrum broadening and energy leakage.
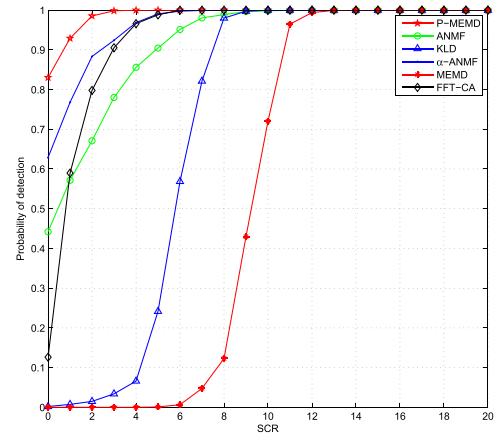

FIGURE 8. The detection performance comparison of P-MEMD, ANMF, α-ANMF, KLD, MEMD and FFT-CA methods in the scenario with energy leakage and no clutter spectrum broadening.
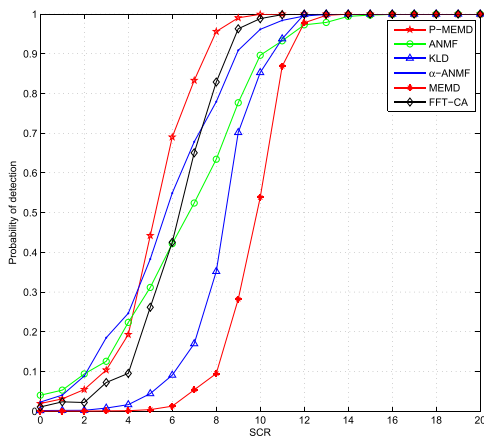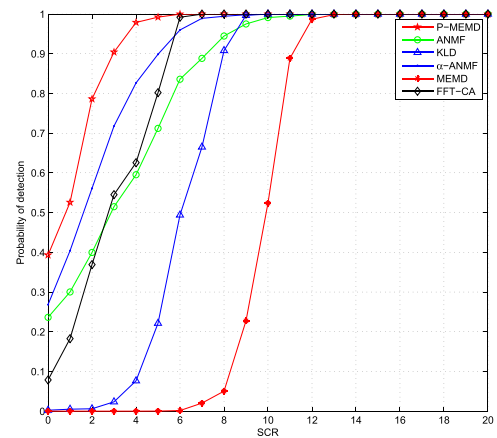

FIGURE 7. The detection performance comparison of P-MEMD, ANMF, α-ANMF, KLD, MEMD and FFT-CA methods in the scenario with clutter spectrum broadening and no energy leakage.

FIGURE 9. The detection performance comparison of P-MEMD, ANMF, α-ANMF, KLD, MEMD and FFT-CA methods in the scenario with energy leakage and clutter spectrum broadening.

and energy leakage. Typically, the detection performance gap between the P-MEMD and MEMD method is increased about 2.7 dB due to the clutter suppression process. However, the detection performance of P-MEMD method is inferior to α-ANMF and ANMF methods when SCR is less than 7dB and 3dB, respectively.

Fig. 7 describes the detection performance comparison curves of P-MEMD, ANMF, α-ANMF, KLD, MEMD and FFT-CA methods in the scenario with clutter spectrum broadening and no energy leakage. Compared with Fig. 6, the detection performance of all the methods are degraded due to clutter spectrum broadening. Nevertheless, the proposed P-MEMD method outperforms than the other methods when the SCR is greater than 5dB.

The detection performance of P-MEMD, ANMF, α-ANMF, KLD, MEMD and FFT-CA methods for the case of energy leakage and the absence of clutter spectrum broadening is shown in Fig. 8. It can be observed from Fig. 8 that the detection performance of several methods are different when the target Doppler frequency removes from the clutter spectrum. Hence, the detection performance of P-MEMD, ANMF, α-ANMF, and KLD methods are greatly improved

due to the little influence of clutter on the detection performance. Moreover, the detection performance of MEMD method is less improved because it cannot compensate the phase fluctuation resulting in low integration gain.

For scenario 4, the detection performance of several methods are compared in Fig. 9. The results show that several methods suffer from performance loss for the case of the clutter spectrum broadening. Nevertheless, the proposed method obtains performance improvement of 1.8 dB over α-ANMF in the case of (4). And it outperforms than ANMF method about 3.9dB.

We also compare the detection probabilities of several methods under different SCRs when the clutter spectrum overlaps with the target spectrum. As shown in Fig. 10, the performance of ANMF, α-ANMF, KLD and FFT-CA methods are degraded when the target Doppler frequency is close to the peak frequency of clutter power spectrum. The performance gap between the proposed method and other methods is increased in the area of strong clutter, which further illustrates the superiority of the proposed method. The main reason for the improvement of detection performance is the clutter is effectively suppressed.
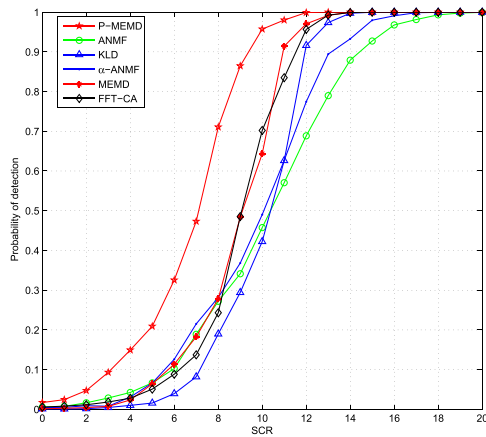
FIGURE 10. The detection performance comparison of P-MEMD, ANMF, α-ANMF, KLD, MEMD and FFT-CA methods in the scenario in which the target spectrum overlaps with the clutter spectrum.
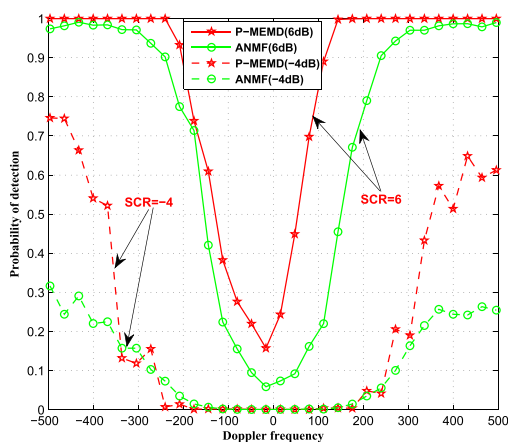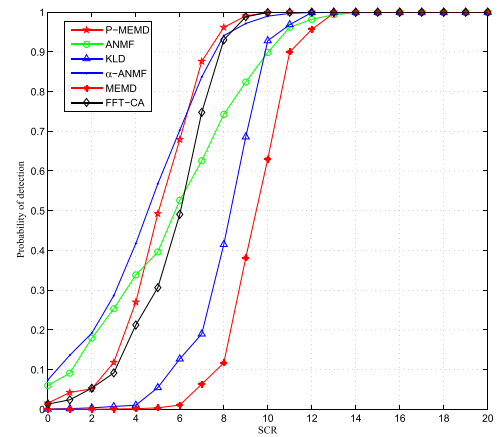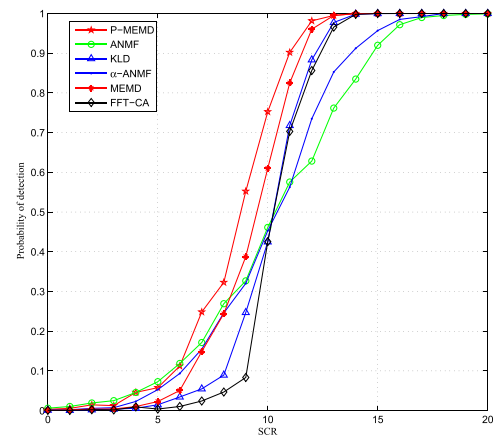

FIGURE 11. Detection performance comparison of P-MEMD and ANMF for different Doppler frequency.


(a) $f_d = 142$ Hz, $3dB = 40$Hz


(b) $f_d = 65$ Hz, $3dB = 80$Hz

FIGURE 12. Detection performance comparison of P-MEMD method and ANMF, α-ANMF, MEMD, KLD and FFT-CA for the scenario with respect to secondary target.

In addition, the actual scenario where the target Doppler frequency is unknown is considered to detect the target within the given Doppler interval of -500 to 500 Hz. The performance comparisons of P-MEMD method and the ANMF method is carried out for the SCR of 6dB and -4dB, respectively. Fig. 11 shows that the proposed method achieves detection performance improvement over ANMF under different Doppler frequency due to the filtering process.

In what follows, the scenario with the presence of secondary targets is considered to verify the robustness of the proposed method. The simulation results with respect to the multiple interfering targets are shown in Fig. 12(a) and Fig. 12(b), respectively. Here, the interference-to-clutter ratio (ICR) is equal to SCR. Fig. 12(a) shows the detection performance comparison of several methods under the condition that target spectrum is non-overlapping with the clutter spectrum ($f_d = 142$ Hz). Fig. 12(b) describes the detection performance comparison of several methods under the condition that target spectrum is overlapped with the clutter spectrum ($f_d = 65$ Hz). As shown in Fig. 12(a) and Fig. 12(b), detection performance of P-MEMD method outperforms than aforementioned detection methods for the scenario with

secondary targets, which indicates the robustness of the proposed method.

In practical scene, the scenario with mismatched steering vector is often encountered due to the influence of array calibration error and multi-path effect. Therefore, this paper considers the detection scenario with mismatched steering vector in order to verify the robustness of P-MEMD method. Here, we consider the mismatched case where the difference between the actual Doppler phase and the nominal Doppler phase is 5°. The receiver-operating-characteristic (ROC) curve gives an overall assessment of a detector over different false alarm rates. In general, the area under the ROC curve (AUROC) is a quantitative index to assess the detection performance of detectors. Detection probability below 0.5 is not enough to form a stable trace of a target for most radars [14]. Therefore, the AUROC where detection probability is over 0.5 is employed to evaluate all the detection methods. Fig. 13(a) describes the comparison of ROC curves of several methods under the condition that the target spectrum is overlapped with the clutter spectrum (nominal target Doppler frequency is $f_d = 65$ Hz). While Fig. 13(b) shows the comparison of ROC curves of several methods
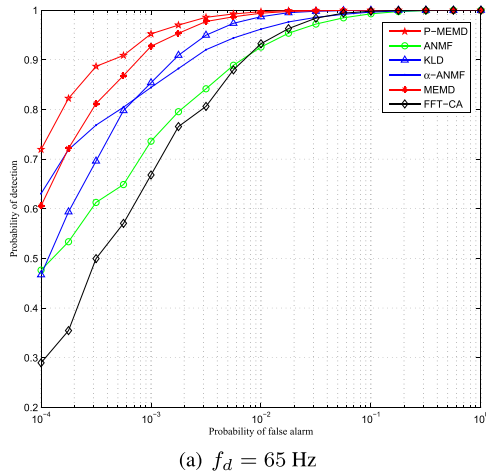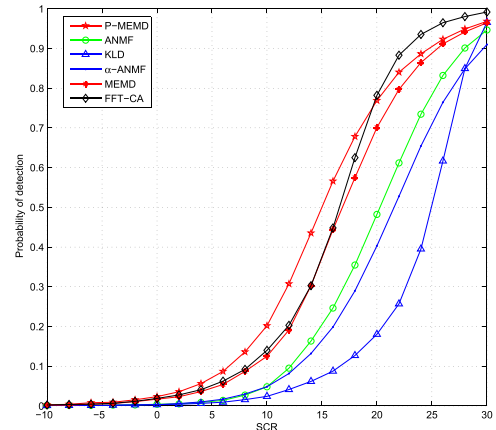
(a) $f_d = 65$ Hz
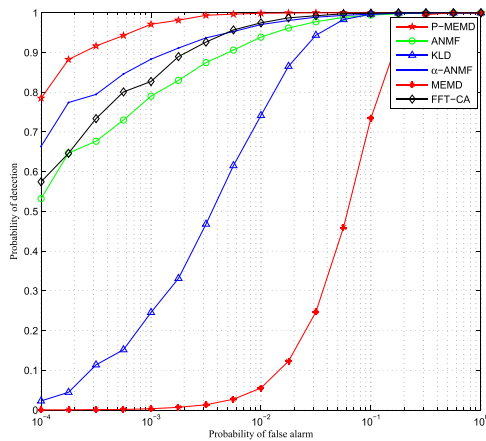
(b) $f_d = 215$ Hz

FIGURE 13. ROC comparison curves of P-MEMD, ANMF, α-ANMF, KLD, MEMD and FFT-CA method for the scenario with mismatched steering vector.

(a) $f_d = 68$ Hz

(b) $f_d = 215$ Hz

FIGURE 14. Detection performance comparison of P-MEMD, ANMF, α-ANMF, KLD, MEMD and FFT-CA method for the real clutter data: 25#19931108_213827_*starea.*
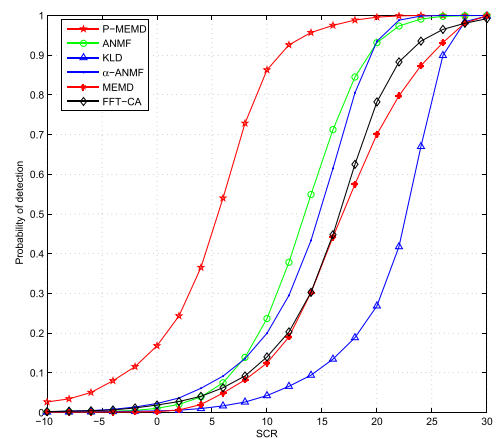
for the scenario where the target spectrum is separated from the clutter spectrum (nominal target Doppler frequency is $f_d = 215$ Hz). In Fig. 13(a) and Fig. 13(b), the SCR is set to be 10 dB and 3 dB, respectively. The other parameters setting are the same as that in the case of (4) and (5). As observed from Fig. 13(a) and Fig. 13(b), the AUROC of P-MEMD method is larger than the others. We can conclude that the detection performance of the proposed P-MEMD method is superior to the ANMF, α-ANMF, MEMD, KLD and FFT-CA methods for the case of mismatched steering vector. The ROC curves further demonstrate the effectiveness of P-MEMD method.

B. SIMULATION EXPERIMENTS ON REAL SEA CLUTTER DATA

Some simulation experiments based on the real clutter data are performed to compare and evaluate the detection performance of P-MEMD and several aforementioned detection methods. The IPIX radar database [44] (file 1: 25#19931108_213827_*starea*) and [45] (file 2: 19980205_185111_*ANTSTEP.CDF*) are employed, which are provided by McMaster university in Canada. The data 1 was collected in 1993 conducted at a site in Osborne Head Gunnery

Range (OHGR), Dartmouth, Nova Scotia, on the East Coast of Canada. The data 2 was collected in 1998 conducted at Grimsby on the shores of Lake Ontario. The data of file 1 was divided into 14 range cells, and the data length in each cell is 131,072. The data of file 2 is composed of 27 range cells, each contains 60,000 clutter data. The shape parameters of K distribution of the two datasets are estimated to be 0.5072 and 1.0563, respectively. The mean Doppler frequencies of sea clutter are estimated about 68 Hz and -204 Hz for two datasets. The false alarm probability is set to be 10^{-3} due to the limited available pulses. Two scenarios in which target spectrum is within clutter spectrum and target Doppler frequency is outside clutter spectrum are considered. For file 1, the target Doppler frequency are set to be 68 Hz and 215 Hz, respectively. While for file 2, the target Doppler frequency are set to be -204 Hz and 215 Hz, respectively.

Fig. 14 (a) and Fig. 15 (a) correspond to the detection scenario where the clutter spectrum overlaps with the target spectrum. The performance of the P-MEMD method is superior to ANMF, α-ANMF, KLD and MEMD methods for these two sea clutter datasets. For X-band radar, slow moving target with target Doppler frequency of 68Hz is detected, whose
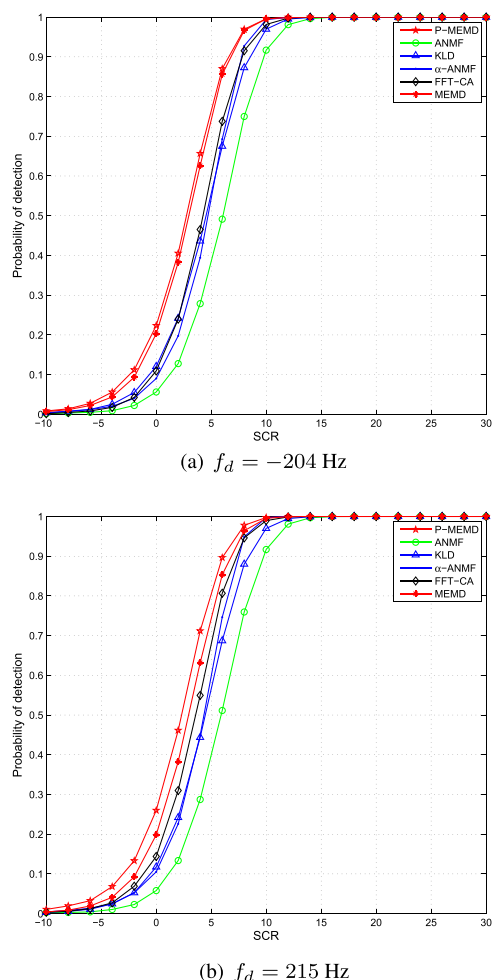
(a) $f_d = -204$ Hz

(b) $f_d = 215$ Hz

FIGURE 15. Detection performance comparison of P-MEMD, ANMF, α-ANMF, KLD, MEMD and FFT-CA method for the real clutter data: **19980205_185111_ANTSTEP.CDF**.

detection probability curve is depicted in Fig. 14 (a). Since the target Doppler frequency is near the center of the filter bank, so there is no energy leakage. And it is almost imperceptible to clutter for the case of $SCR > 20$, FFT-CA method is more favorable to detect targets by using the total energy of received signals for the scenario where the target spectrum overlaps with the clutter spectrum, so it has slightly higher performance than the proposed algorithm that only uses the maximum eigenvalue for $SCR > 20$. It is worth noting that the P-MEMD method achieves the performance improvement of 1.2 dB over MEMD method in Fig. 14(a), which further indicates that the P-MEMD method can effectively improve detection performance by making full use of the phase information. Fig. 14 (b) and Fig. 15 (b) describe the detection performance comparison under the condition that the target Doppler frequency removes from the clutter spectrum. The detection performance of P-MEMD, ANMF, α-ANMF, and KLD are improved with the increase of target Doppler frequency. However, the performance of FFT-CA is degraded due to energy leakage. Several simulation experiments based on real clutter data indicate that the proposed P-MEMD

method is more robust than other algorithms.

In conclusion, P-MEMD method yields robust performance in different detection scenarios. It outperforms the other algorithms in the case of matched and mismatched target Doppler steering vector. Hence, the P-MEMD method is more suitable for practical applications from the perspective of detection capability.

V. CONCLUSION
This paper provides a pre-processing based maximum eigenvalue detection method to the problem of detecting moving target under sea clutter environment. The proposed method utilizes the priori information of target Doppler steering vector to suppress the clutter as well as improve the detection performance. In particular, the proposed detector possesses the CFAR property with respect to clutter covariance matrix. This paper considers five detection scenarios including energy leakage, clutter spectrum broadening and overlap between the spectrum and the target spectrum. The simulation results show that the proposed method has not only good detection performance in the strong clutter environment, but also the scenario where the target Doppler frequency removes from the clutter spectrum. In addition, the proposed method also achieves better detection performance for the case with mismatched target steering vector and multiple interfering targets. In the future research, the mathematical mechanism of P-MEMD method to achieve superior detection performance will be theoretically analyzed.

REFERENCES
[1] X. Chen, J. Guan, Y. Huang, N. Liu, and Y. He, "Radon-linear canonical ambiguity function-based detection and estimation method for marine target with micromotion," *IEEE Trans. Geosci. Remote Sens.*, vol. 53, no. 4, pp. 2225–2240, Apr. 2015.
[2] X. Chen, B. Chen, Y. Huang, Y. He, and J. Guan, "Space-range-Doppler focus-based low-observable moving target detection using frequency diverse array MIMO radar," *IEEE Access*, vol. 6, pp. 43892–43904, 2018.
[3] Y. Liu, S. Zhang, J. Suo, J. Zhang, and T. Yao, "Research on a new comprehensive CFAR (Comp-CFAR) processing method," *IEEE Access*, vol. 7, pp. 19401–19413, 2019.
[4] F. Barbaresco, T. Forget, E. Chevallier, and J. Angulo, "Doppler spectrum segmentation of radar sea clutter by mean-shift and information geometry metric," in *Proc. 17th Int. Radar Symp. (IRS)*, Krakow, Poland, May 2016, pp. 1–6.
[5] F. Barbaresco, "Innovative tools for radar signal processing based on Cartan's geometry of SPD matrices & information geometry," in *Proc. IEEE Radar Conf.*, Rome, Italy, May 2008, pp. 1–6.
[6] J. A. Scheer and W. L. Melvin, *Principles of Modern Radar*. Rijeka, Croatia: SciTech, 2010.
[7] M. A. Richards, *Fundamentals of Radar Signal Processing*, 2nd ed. New York, NY, USA: McGraw-Hill, 2014.
[8] F. C. Robey, D. R. Fuhrmann, E. J. Kelly, and R. Nitzberg, "A CFAR adaptive matched filter detector," *IEEE Trans. Aerosp. Electron. Syst.*, vol. 28, no. 1, pp. 208–216, Jan. 1992.
[9] E. Conte, M. Lops, and G. Ricci, "Asymptotically optimum radar detection in compound-Gaussian clutter," *IEEE Trans. Aerosp. Electron. Syst.*, vol. 31, no. 2, pp. 617–625, Apr. 1995.
[10] F. Gini, "Sub-optimum coherent radar detection in a mixture of K-distributed and Gaussian clutter," *IEE Proc.-Radar, Sonar Navigat.*, vol. 144, no. 1, pp. 39–48, Feb. 1997.
[11] E. Conte, M. Lops, and G. Ricci, "Adaptive detection schemes in compound-Gaussian clutter," *IEEE Trans. Aerosp. Electron. Syst.*, vol. 34, no. 4, pp. 1058–1069, Oct. 1998.

[12] G. Cui, N. Li, L. Pallotta, G. Foglia, and L. Kong, "Geometric barycenters for covariance estimation in compound-Gaussian clutter," *IET Radar, Sonar Navigat.*, vol. 11, no. 3, pp. 404–409, 2017.

[13] F. Bandiera, O. Besson, and G. Ricci, "Knowledge-aided covariance matrix estimation and adaptive detection in compound-Gaussian noise," *IEEE Trans. Signal Process.*, vol. 58, no. 10, pp. 5391–5396, Oct. 2010.

[14] P.-L. Shui, M. Liu, and S.-W. Xu, "Shape-parameter-dependent coherent radar target detection in K-distributed clutter," *IEEE Trans. Aerosp. Electron. Syst.*, vol. 52, no. 1, pp. 451–465, Feb. 2016.

[15] R. Raghavan, "Analysis of steering vector mismatch on adaptive noncoherent integration," *IEEE Trans. Aerosp. Electron. Syst.*, vol. 49, no. 4, pp. 2496–2508, Oct. 2013.

[16] J. Liu, W. Liu, B. Chen, H. Liu, and H. Li, "Detection probability of a CFAR matched filter with signal steering vector errors," *IEEE Signal Process. Lett.*, vol. 22, no. 12, pp. 2474–2478, Dec. 2015.

[17] I. Ben Atitallah, A. Kammoun, M.-S. Alouini, and T. Y. Al-Naffouri, "Optimal design of large dimensional adaptive subspace detectors," *IEEE Trans. Signal Process.*, vol. 64, no. 19, pp. 4922–4935, Oct. 2016.

[18] T. Jian, F. Su, Y. He, C.-W. Qu, and B. Zhang, "Performance assessment of range-spread target detector for unwanted signal in non-Gaussian clutter," *ACTA Electronica Sinica*, vol. 38, no. 7, pp. 1478–1482, 2010.

[19] M. Arnaudon, F. Barbaresco, and L. Yang, "Riemannian medians and means with applications to radar signal processing," *IEEE J. Sel. Topics Signal Process.*, vol. 7, no. 4, pp. 595–604, Aug. 2013.

[20] X. Zhao and S. Wang, "An improved matrix CFAR detection method base on KL divergence," *J. Electron. Inf. Technol.*, vol. 38, no. 4, pp. 934–940, Apr. 2016.

[21] H. Hua, Y. Cheng, H. Wang, Y. Qin, Y. Li, and W. Zhang, "Matrix CFAR detectors based on symmetrized Kullback–Leibler and total Kullback–Leibler divergences," *Digit. Signal Process.*, vol. 69, pp. 106–116, Oct. 2017.

[22] X. Hua, Y. Cheng, H. Wang, Y. Qin, and Y. Li, "Geometric means and medians with applications to target detection," *IET Signal Process.*, vol. 11, no. 6, pp. 711–720, 2017.

[23] W. Zhao, C. Liu, W. Liu, and M. Jin, "Maximum eigenvalue-based target detection for the K-distributed clutter environment," *IET Radar, Sonar Navigat.*, vol. 12, no. 11, pp. 1294–1306, Nov. 2018.

[24] W. Zhao, M. Jin, and W. Liu, "A modified matrix CFAR detector based on maximum eigenvalue for target detection in the sea clutter," in *Proc. IEEE Radar Conf. (RadarConf)*, Oklahoma, OK, USA, Apr. 2018, pp. 0896–0901.

[25] K. D. Ward, R. J. A. Tough, and S. Watts, *Sea Clutter: Scattering, the K Distribution and Radar Performance*, 2nd ed. London, U.K.: IET, 2013.

[26] F. Gini and A. Farina, "Vector subspace detection in compound-Gaussian clutter. Part I: Survey and new results," *IEEE Trans. Aerosp. Electron. Syst.*, vol. 38, no. 4, pp. 1295–1311, Oct. 2002.

[27] G. Weinberg, *Radar Detection Theory of Sliding Window Processes*. Boca Raton, FL, USA: CRC Press, 2017.

[28] S. Wang, Y. Wan, and J. Liu, *Modern Radar Target Detection Theory and Method*. Beijing, China: Science Press, 2015.

[29] R. Inkol, S. Wang, and S. Rajan, "FFT filter bank-based CFAR detection schemes," in *Proc. 50th Midwest Symp. Circuits Syst.*, Montreal, QC, Canada, Aug. 2007, pp. 409–412.

[30] E. Conte, and A. De Maio, "Exploiting persymmetry for CFAR detection in compound-Gaussian clutter," *IEEE Trans. Aerosp. Electron. Syst.*, vol. 39, no. 2, pp. 719–724, Apr. 2003.

[31] F. Pascal, Y. Chitour, J.-P. Ovarlez, P. Forster, and P. Larzabal, "Covariance structure maximum-likelihood estimates in compound Gaussian noise: Existence and algorithm analysis," *IEEE Trans. Signal Process.*, vol. 56, no. 1, pp. 34–48, Jan. 2008.

[32] H. Harari-Kermadec and F. Pascal, "On the use of empirical likelihood for non-Gaussian clutter covariance matrix estimation," in *Proc. IEEE Radar Conf.*, May 2008, pp. 1–6.

[33] I. Soloveychik, and A. Wiesel, "Tyler's covariance matrix estimator in elliptical models with convex structure," *IEEE Trans. Signal Process.*, vol. 62, no. 20, pp. 5251–5259, Oct. 2014.

[34] A. De Maio, D. Orlando, I. Soloveychik, and A. Wiesel, "Invariance theory for adaptive detection in interference with group symmetric covariance matrix," *IEEE Trans. Signal Process.*, vol. 64, no. 23, pp. 6299–6312, Dec. 2016.

[35] J. Guan, Y.-N. Peng, and Y. He, "Proof of CFAR by the use of the invariant test," *IEEE Trans. Aerosp. Electron. Syst.*, vol. 36, no. 1, pp. 336–339, Jan. 2000.

[36] A. Ghobadzadeh, S. Gazor, M. R. Taban, A. A. Tadaion, and S. M. Moshtaghioun, "Invariance and optimality of CFAR detectors in binary composite hypothesis tests," *IEEE Trans. Signal Process.*, vol. 62, no. 14, pp. 3523–3535, Jul. 2014.

[37] E. Conte, A. D. Maio, and G. Ricci, "Covariance matrix estimation for adaptive CFAR detection in compound-Gaussian clutter," *IEEE Trans. Aerosp. Electron. Syst.*, vol. 38, no. 2, pp. 415–426, Apr. 2002.

[38] E. Conte, A. De Maio, and C. Galdi, "CFAR detection of multidimensional signals: An invariant approach," *IEEE Trans. Signal Process.*, vol. 51, no. 1, pp. 142–151, Jan. 2003.

[39] H. Li and J. Wen, "A new analysis for support recovery with block orthogonal matching pursuit," *IEEE Signal Process. Lett.*, vol. 26, no. 2, pp. 247–251, Feb. 2019.

[40] H. Li, L. Wang, X. Zhan, and D. K. Jain, "On the fundamental limit of orthogonal matching pursuit for multiple measurement vector," *IEEE Access*, vol. 7, pp. 48860–48866, 2019.

[41] J. Wen and X. W. Chang, "On the KZ reduction," *IEEE Trans. Inf. Theory.*, vol. 65, no. 3, pp. 1921–1935, Mar. 2019.

[42] J. Wen, Z. Zhou, Z. Liu, M.-J. Lai, and X. Tang, "Sharp sufficient conditions for stable recovery of block sparse signals by block orthogonal matching pursuit," *Appl. Comput. Harmon. Anal.*, to be published.

[43] A. Aubry, A. D. Maio, and L. Pallotta, "A geometric approach to covariance matrix estimation and its applications to radar problems," *IEEE Trans. Signal Process.*, vol. 66, no. 4, pp. 907–922, Feb. 2018.

[44] IPIX radar file. (1993). *IPIX Radar Dataset Files in Dartmouth*. [Online]. Available: http://soma.ece.mcmaster.ca/ipix/dartmouth/cdfhowto.html

[45] IPIX radar file. (2003). *IPIX Radar Dataset Files in Grimsby on the Shores of Lake Ontario*. [Online]. Available: http://soma.mcmaster.ca/ipix.php
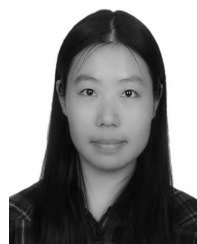
WENJING ZHAO was born in Liaoning, China, in 1990. She received the B.S. degree in mathematics and applied mathematics from Liaoning Normal University, in 2012, the M.S. degrees in fundamental mathematics from Northeast Normal University, Changchun, China, in 2015. She is currently pursuing the Ph.D. degree in information and communication engineering with the Dalian University of Technology, Dalian, China.

Her current research interests include information geometry, statistical Signal processing, and radar target detection.

MINGLU JIN (M'96) received the B.S. degree from the University of Science and Technology of China, Hefei, China, in 1982, the M.S. and Ph.D. degrees from the Beijing University of Aeronautics and Astronautics, Beijing, China, in 1984 and 1995, respectively.

He was a Visiting Scholar with Arimoto Laboratory, Osaka University, Osaka, Japan, from 1987 to 1988. He was a Research Fellow with Radio and Broadcasting Research Laboratory, Electronics Telecommunications Research Institute, Daejeon, South Korea, from 2001 to 2004. He is currently a Professor with the Dalian University of Technology, Dalian, China.

His research interests include wireless communication, wireless sensor networks, and signal processing for wireless communication system.

• • •